

TABLE 3  
ABSORBENTS SCREENED FOR H<sub>2</sub>S REMOVAL

<u>Adsorbent</u>	<u>Manufacturer</u>	<u>Type</u>
H-7	Linde	Zeolite
CaX	LaPorte	Ca exchanged X zeolite
BPL	Calgon	Activated carbon
FCA	Calgon	CuO/Ca <sub>2</sub> O <sub>3</sub> loaded Activated carbon
Desulf 8	Calgon	CuO loaded Activated carbon
EPJ-19	UCI	MeOH catalyst
BASF S3-85	BASF	MeOH catalyst
HTZ-4	Haldror-Topsoe	Promoted ZuO

FIGURE 22

# Effect of Temperature on COS Adsorption 90 psig on FCA carbon

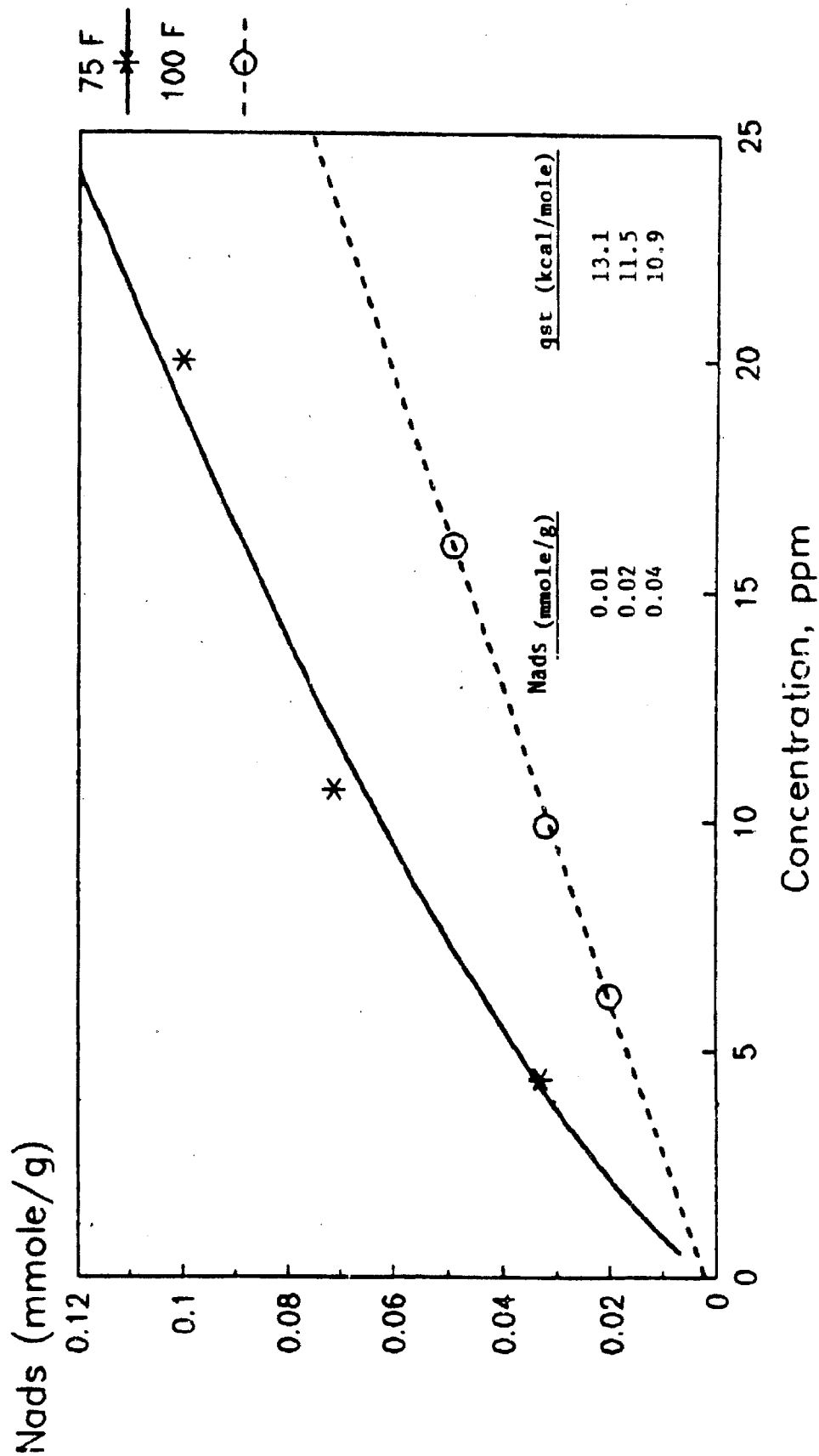


Figure 23 gives the  $H_2S$  adsorption isotherms on BPL, H-Y, CaX, HTZ-4, and 10% MgO on BPL. Interestingly, HTZ-4 shows significant  $H_2S$  capacity even at this low temperature, however, this capacity is not regenerable. Of the two zeolite adsorbents, H-Y yields a higher  $H_2S$  capacity than CaX. Even though  $H_2S$  is a polar adsorbate and CaX is a more polar adsorbent than H-Y, H-Y has a higher  $H_2S$  capacity under the conditions investigated. This is because the primary carrier gas,  $CO_2$ , is also a polar molecule which interacts more strongly with CaX than H-Y thereby reducing the capacity of CaX. Figure 23 also shows a comparison of  $H_2S$  adsorption on BPL carbon and 10% MgO on BPL carbon. The impregnation of a basic metal oxide like MgO on the surface of the carbon clearly increases the  $H_2S$  capacity. This can be explained as an acid-base interaction between MgO and acidic  $H_2S$ .

Figure 24 gives trace  $H_2S$  adsorption isotherms on the other adsorbents screened. These adsorbents all demonstrate enhanced  $H_2S$  capacity over the previous adsorbents. The highest  $H_2S$  capacities measured are for the two spent MeOH catalysts. BASF S3-85 shows the highest  $H_2S$  capacity (about 5 mmole/g at 2 ppm), which is about twice that of EPJ-19. The rectangular isotherm shape suggests a chemisorptive process occurs with these materials. The very high  $H_2S$  capacity of these spent catalysts indicate that they may be useful throw-away adsorbents. The  $H_2S$  capacities of the other two adsorbents, FCA and desulf-12, are lower than those for spent catalyst but still quite high. The  $H_2S$  capacity of FCA at 5 ppm is about 1.3 mmole/g and the corresponding value for desulf 12 is about 0.7 mmole/g. The advantage of using these materials for  $H_2S$  removal is that they are both steam regenerable. Hence, these adsorbents could be employed in a steam regenerated TSA system for  $H_2S$  removal. One final point of interest is that all four

FIGURE 23

# H<sub>2</sub>S Adsorption on Various Adsorbents 75 F and 90 psig

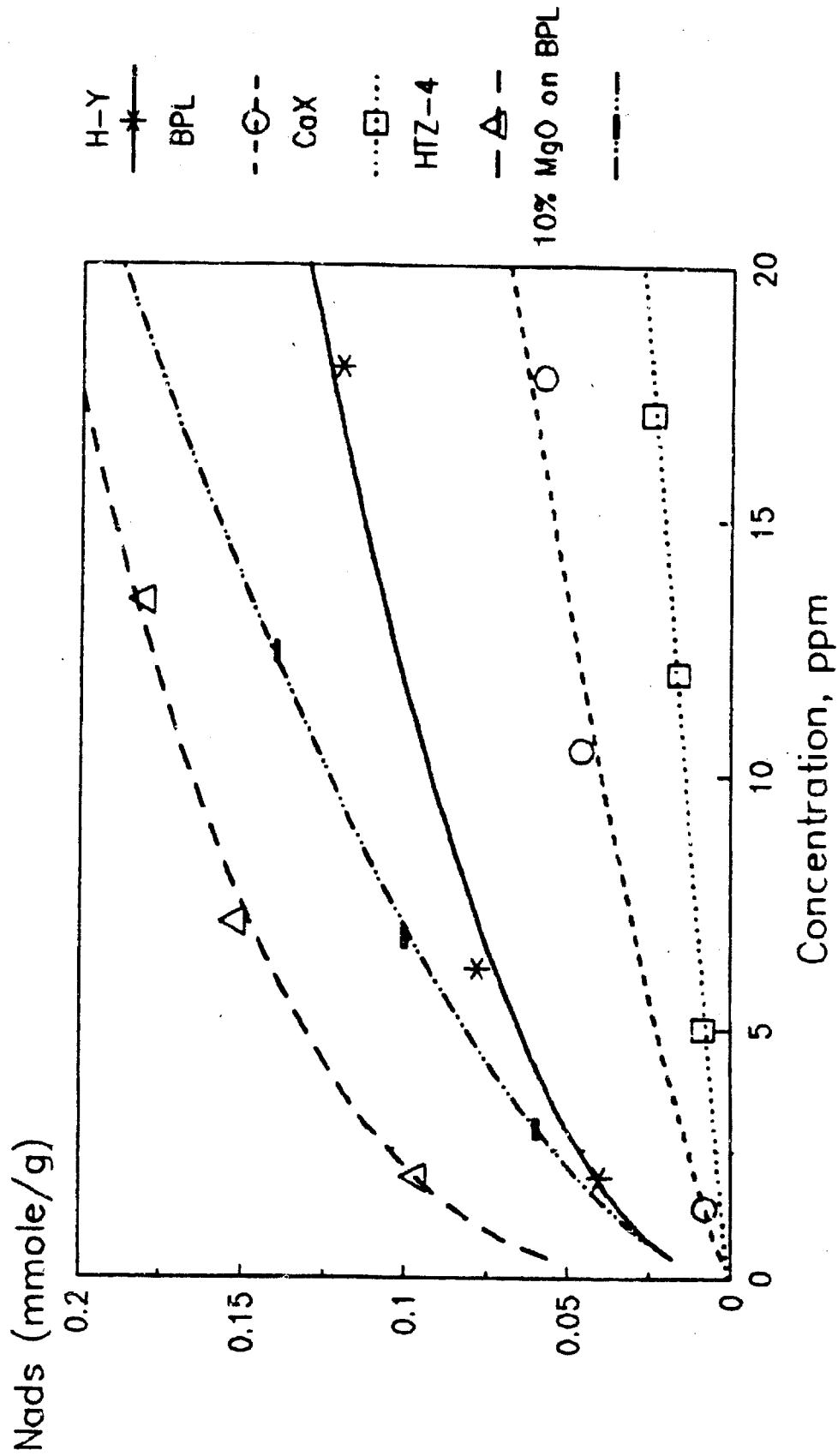
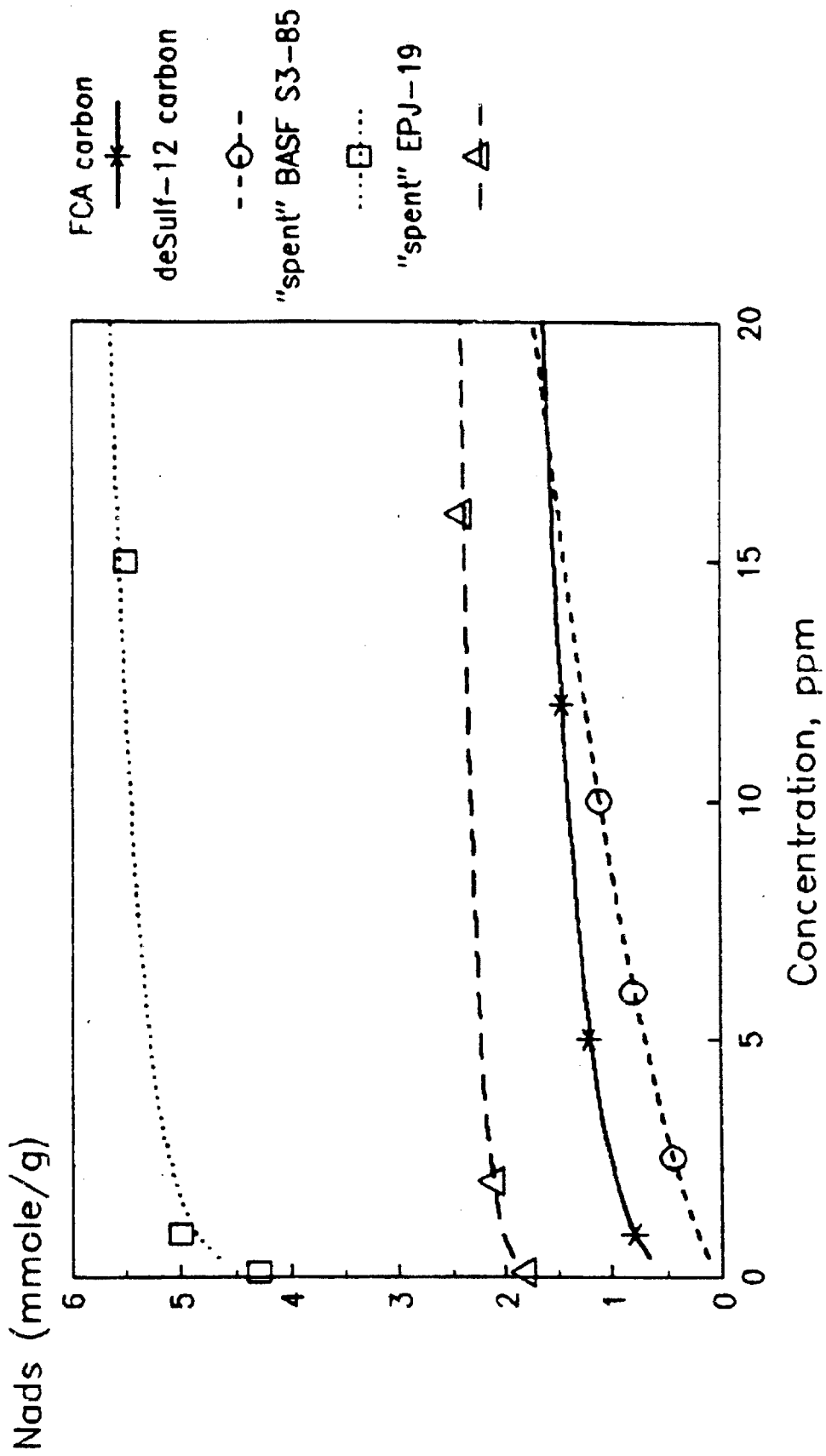


FIGURE 24

# H<sub>2</sub>S Adsorption on Various Adsorbents 75 F and 90 psig



adsorbents shown in Figure 24 demonstrate high  $H_2S$  capacity and all contain copper. Thus, it may be expected that other copper containing materials, e.g., shift catalyst, will also have high  $H_2S$  capacities.

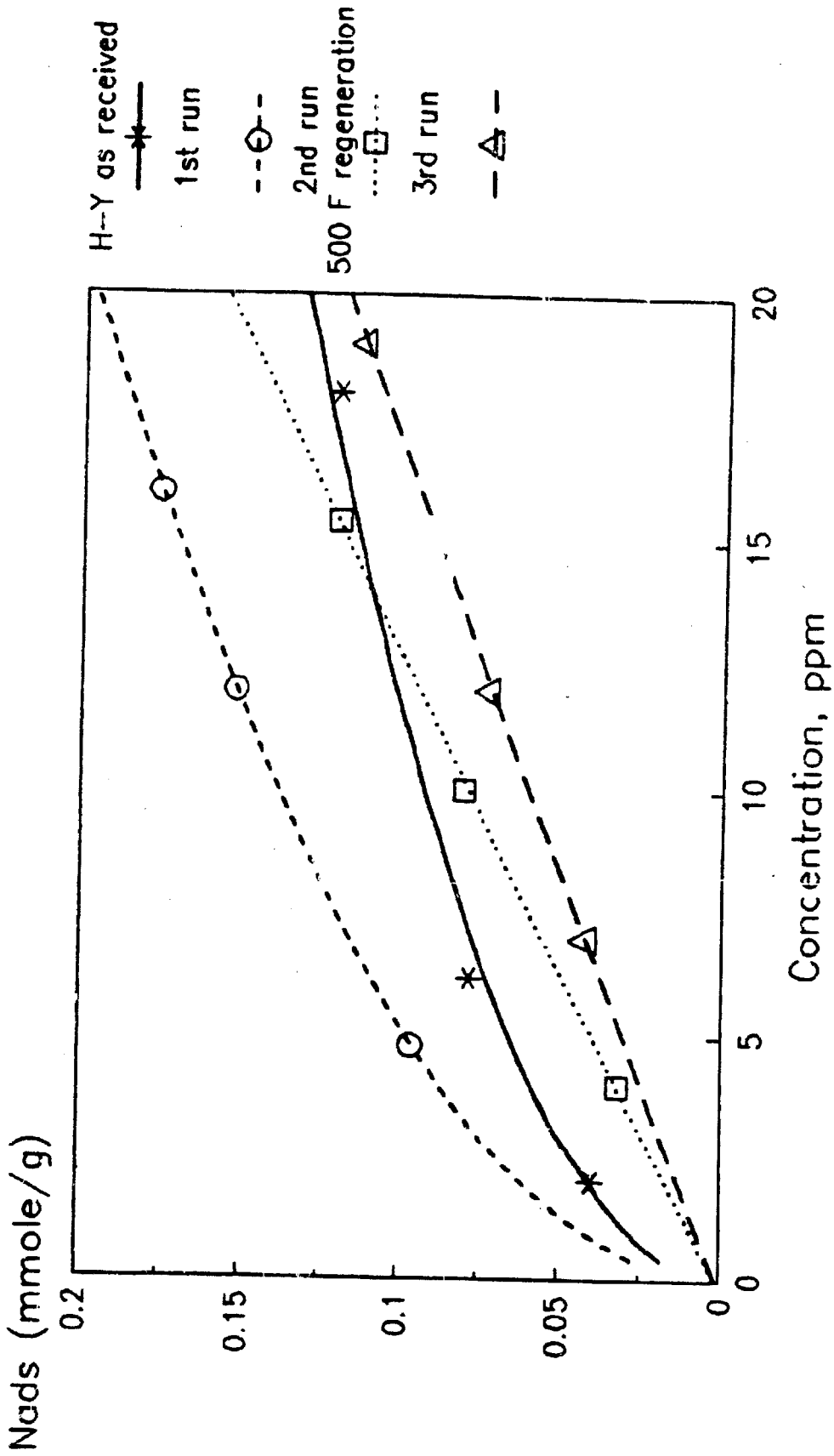
Another point to be made concerning  $H_2S$  removal using steam regenerable adsorbents like FCA carbon is that these materials are best suited for  $H_2S$  removal at low inlet  $H_2S$  concentrations. Looking at the isotherm for FCA in Figure 24 shows the  $H_2S$  capacity at 2 ppm is about equal to that at 10 ppm due to the rectangular isotherm shape. Thus, as the inlet  $H_2S$  concentration increases, the total  $H_2S$  needed to be processed increases, but the capacity remains relatively constant. Clearly, rectangular isotherm shapes are conducive to removing impurities at low inlet concentrations.

#### $H_2S$ Adsorption on Linde H-Y Following $Fe(CO)_5$ Adsorption/Regeneration Cycles

From previous adsorption studies with  $Fe(CO)_5$  it was determined that Linde H-Y may be a better adsorbent for  $Fe(CO)_5$  removal than activated carbon, even though the initial capacity on carbon is greater than that on zeolite. This is because H-Y thermal regeneration is superior to carbon. However, thermal desorption curves and gravimetric analysis indicate that  $Fe(CO)_5$  is decomposed during thermal regeneration leaving iron containing species on the adsorbent surface. The iron species may act as adsorption centers for sulfur containing gases, especially  $H_2S$ . To investigate this possibility,  $H_2S$  adsorption isotherms were measured on a sample of Linde H-Y that had gone through these adsorption/regeneration cycles with  $Fe(CO)_5$ . The iron weight loading on the adsorbent was 33%. Those adsorption isotherms are depicted in Figure 25.

FIGURE 25

# H<sub>2</sub>S Adsorption on Fe(CO)<sub>5</sub> laden H-Y 75 F and 90 psig



The figure shows a number of interesting points. First, the first  $H_2S$  isotherm on the iron contaminated zeolite shows a higher  $H_2S$  capacity than as-received H-Y. This suggests that deposited iron does act as an adsorption site for  $H_2S$ . Second, successive regenerations of this adsorbent at  $500^\circ F$  in  $N_2$  following  $H_2S$  adsorption show a decrease in  $H_2S$  capacity. Presumably, the enhanced  $H_2S$  capacity noted in the first isotherm is due to chemisorption of  $H_2S$ , and this capacity is not recovered by thermal regeneration in  $N_2$ . These data indicate that the interaction between catalyst poisons on thermally regenerated adsorbents is a complex problem and must be considered during poison removal design.

#### Adsorbent Selection for $H_2S$ Removal

The results from  $H_2S$  adsorption measurements indicate that a number of options for  $H_2S$  removal exist. Firstly, it appears that spent MeOH catalyst may provide a good throw-away adsorbent. Unfortunately, the form of the catalyst for LPMeOH production is powdered and a fixed bed adsorber requires some adsorbent with larger particle size. A liquid phase guard bed may, however, be useful. A second option is a regenerable system using type FCA carbon. Regeneration of FCA carbon requires  $500^\circ F$  steam since metallic sulfides from  $H_2S$  chemisorption must be reconverted to metallic oxides.

#### COS and $H_2S$ Removal with Hot Zinc Oxide

Another conventional technology for COS and  $H_2S$  removal is hydrolysis of COS to  $H_2S$  and adsorption/reaction of  $H_2S$  on zinc oxide. To investigate this option for sulfur removal, COS hydrolysis and  $H_2S$  adsorption were measured



at 400°F on an alumina promoted zinc oxide (Haldor Topsoe HTZ-4). The H<sub>2</sub>S capacity of HTZ-4 at 400°F from 90 psig CO<sub>2</sub> was determined to be 3.1 mmole/g or 10.5% by weight. This measured capacity agrees well with the vendor's reported capacity. In addition, the hydrolysis of COS with HTZ-4 was measured at 400°F and 90 psig CO<sub>2</sub> pressure. With an initial concentration of 156 ppm COS and 5000 ppm H<sub>2</sub>O, the COS concentration was reduced to 1 ppm at equilibrium. The corresponding "capacity" was calculated to be 1.8 mmole/g.

Thus, hot promoted zinc oxide provides a viable sulfur removal system. The zinc oxide system provides a number of advantages over the ambient temperature adsorption approach. First, zinc oxide is a throw-away adsorbent so no regeneration system is needed. Second, this promoted zinc oxide works at significantly lower temperature than conventional zinc oxide. Finally, the COS capacity of HTZ-4 is significantly greater than any ambient temperature adsorbent.

It should be emphasized that only equilibrium information on COS and H<sub>2</sub>S removal was obtained. Thus, the MTZ length for H<sub>2</sub>S adsorption is still unknown.

#### Adsorption of HCl

#### Adsorbent Screening

Initial screening of adsorbents for HCl removal was carried out by measuring adsorption isotherms at 75°F from 90 psig carrier (85% CO<sub>2</sub>, 14% N<sub>2</sub>, 1% CO). The adsorbents screened included HY, BPL, Alcoa Selexsorb HCl.

Barneby-Cheney carbons type ST and CH, FCA carbon, and spent methanol catalyst, BASF S3-85.

Figure 26 shows adsorption isotherms on all adsorbents except S3-85. Type FCA carbon demonstrates the highest HCl capacity of those adsorbents depicted followed by type CH carbon. Thus, metal oxide loaded active carbons demonstrate high HCl capacity. The capacity of type FCA carbon at 5 ppm is 1.75 mmole/g or 6.4 wt%. The caustic impregnated carbon, type ST, demonstrates less HCl capacity than the metal oxide impregnated adsorbents. Perhaps unsurprising is that polar adsorbents like H-Y and selexsorb HCl adsorb more HCl than the non-polar active carbon, BPL. The HCl capacity of H-Y is a very respectable 0.40 mmole/g at 5 ppm.

Figure 27 gives the HCl isotherm on spent methanol catalyst BASF S3-85. The spent catalyst demonstrates very large HCl capacity, adsorbing 7.4 mmole/g at an equilibrium concentration of 5 ppm. This large capacity suggests that spent catalyst may be an acceptable throw-away adsorbent for HCl removal.

#### Effect of Thermal Regeneration on FCA Carbon and H-Y Zeolite

The effect of thermal regeneration on HCl capacity was investigated on type FCA carbon and H-Y zeolite. Figure 28 shows HCl adsorption isotherms at 75°F and 90 psig (85% CO<sub>2</sub>/14% CO/1% N<sub>2</sub>) on three successive adsorption/regeneration cycles on FCA carbon. Regeneration was carried out in N<sub>2</sub> at 500°F. As noted, thermal regeneration in N<sub>2</sub> does not restore the HCl capacity of the adsorbent. This suggests that HCl is chemisorbed on FCA carbon. Thus, FCA cannot be used in TSA applications for HCl removal.

FIGURE 26

# HCl Adsorption on Various Adsorbents 75 F and 90 psig

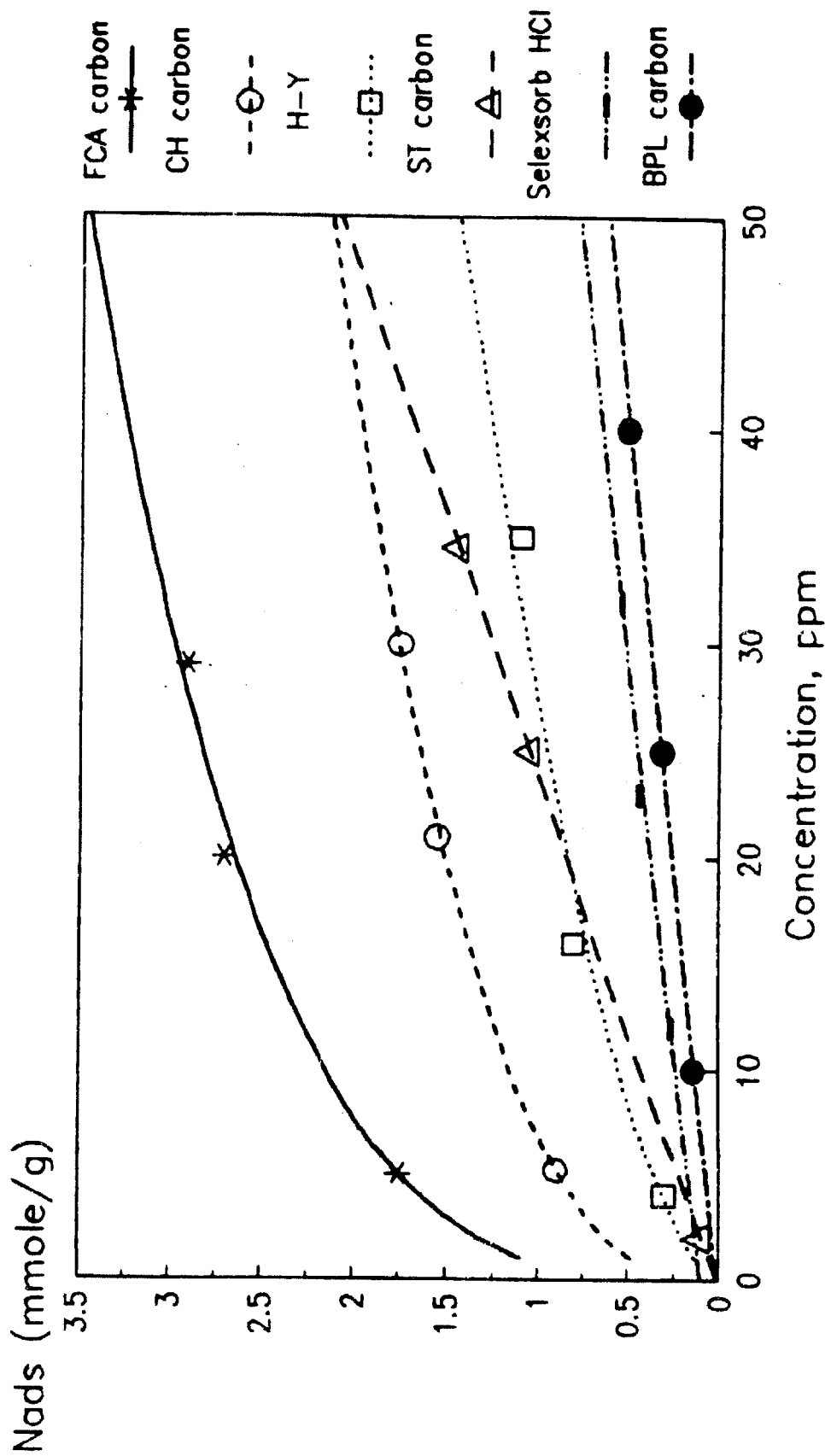


FIGURE 27

# HCl Adsorption on BASF S3-85 75 F and 90 psig

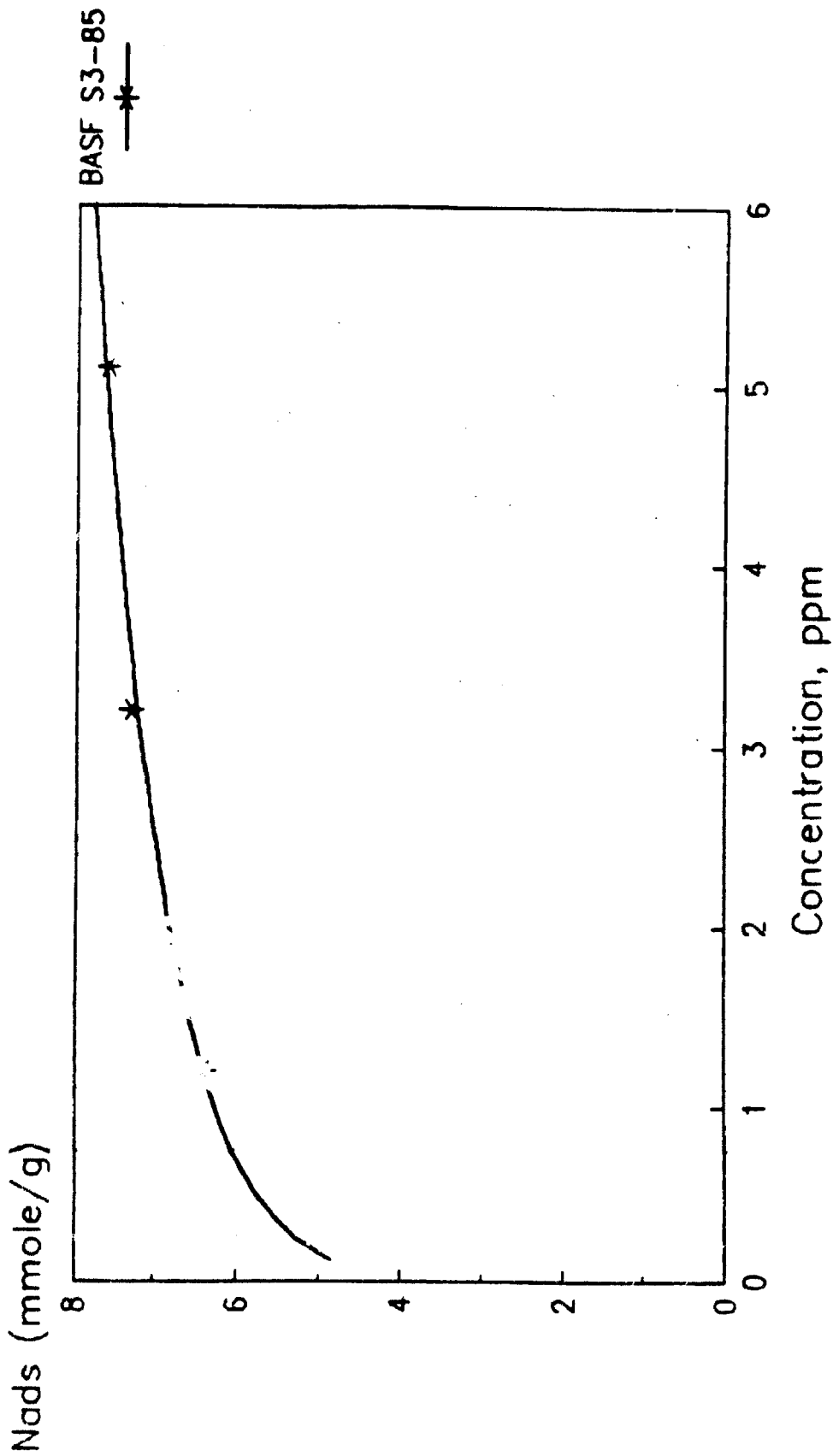


FIGURE 28

# Effect of Thermal Regeneration on HCl Capacity 75 F and 90 psig on FCA carbon

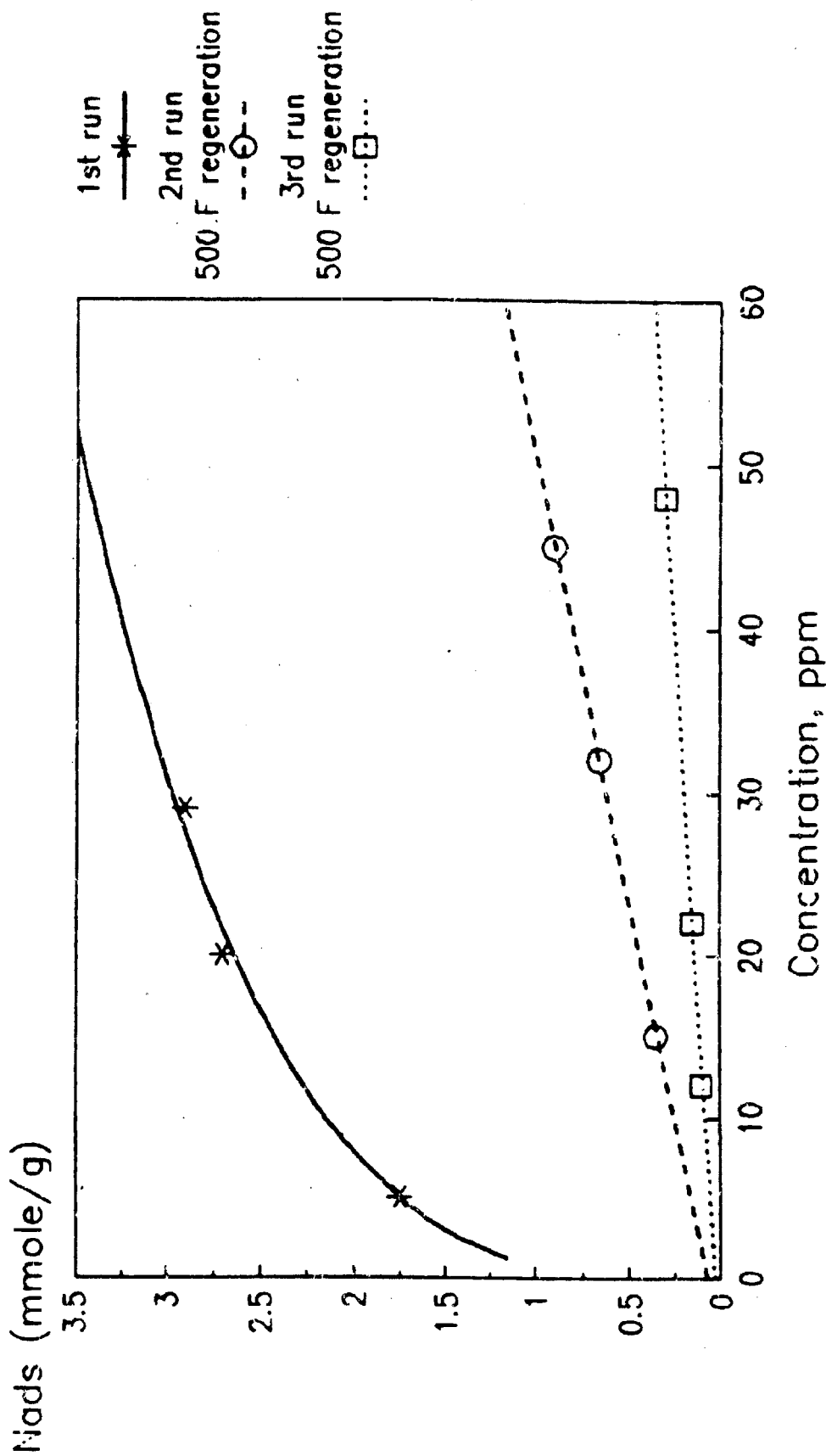


Figure 29 shows the HCl capacity on H-Y zeolite following two adsorption/regeneration cycles, regeneration carried out in N<sub>2</sub> at 500°F. As in the case with FCA carbon, thermal regeneration does not restore the initial HCl capacity. Once again, TSA removal of HCl with H-Y zeolite is not feasible.

#### Effect of Water Loading on HCl Capacity of H-Y Zeolite

Figure 30 shows HCl adsorption isotherms on Linde H-Y with two different water loadings. In general, as the water loading of a zeolite increases, its adsorptive capacity decreases because the water occupies available surface area and pore volume. However, since HCl is quite soluble in water, it was conjectured that the presence of water may in fact increase the HCl capacity. As noted in Figure 30, this is indeed the case. At an equilibrium concentration of 5 ppm, the sample with 0.0% water (regenerated in N<sub>2</sub> at 400°C) demonstrates an HCl capacity of 0.40 mmole/g, while the sample with 7.5% water has a capacity of 0.75 mmole/g. Hence, the presence of water on zeolite enhances its HCl capacity.

#### Adsorbent for HCl Removal

Of those adsorbents screened, the preferred adsorbent for HCl is spent methanol catalyst due to its large capacity. The large capacity, 7.4 mmole/g at 5 ppm, indicates that a throw-away adsorbent for HCl removal is a viable removal technique.

FIGURE 29

# Effect of Thermal Regeneration on HCl Capacity

75 F and 90 psig on H-Y

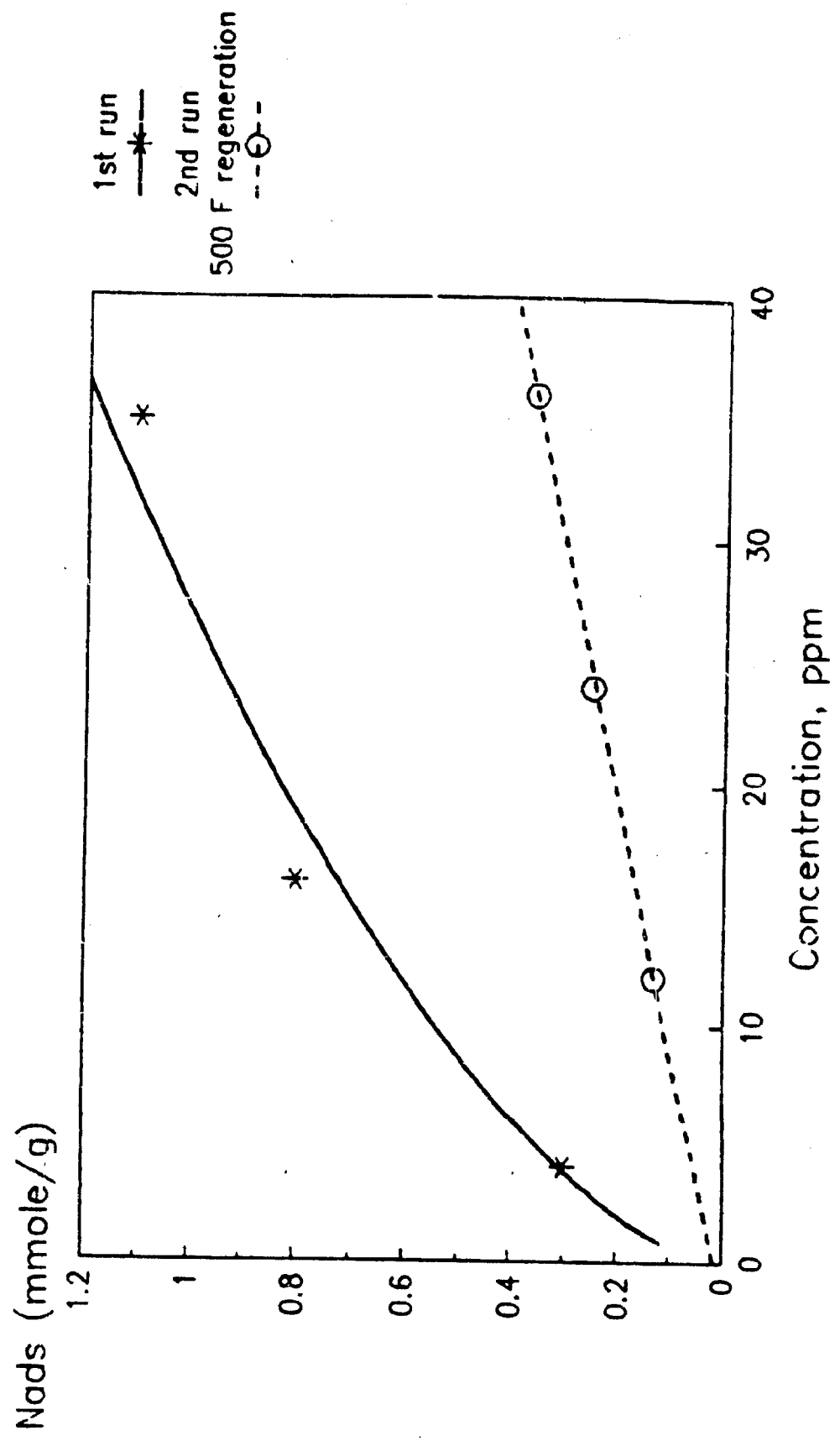
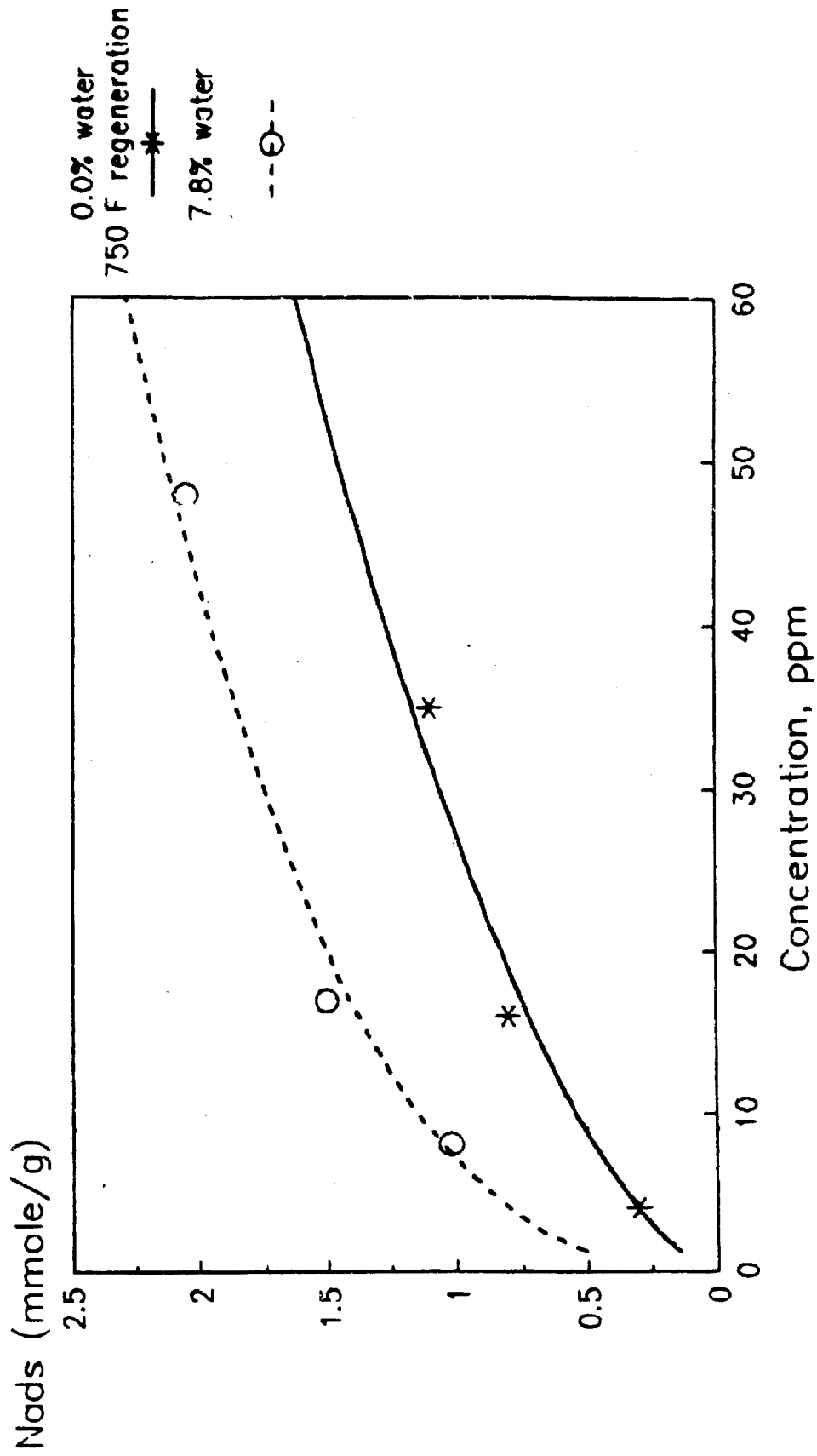


FIGURE 30

# Effect of Water Content on HCl Capacity 75 F and 90 psig on H-Y





## Pilot Unit Design

### Estimation of Mass Transfer Zone Lengths

The design of an adsorption system for removal of catalyst poisons from synthesis gas requires an estimation of the mass transfer zone (MTZ) length required for removal of a given impurity. During the dynamic operation of an adsorber bed, there exists both an equilibrium and non-equilibrium zone in the bed. In the equilibrium zone, the adsorbent is in equilibrium with the trace impurity at its inlet concentration. In the non-equilibrium or mass transfer zone, there exists a gradient in gas phase concentration of the impurity which varies from its inlet concentration to essentially zero. The length of the MTZ depends on many variables including the shape of the adsorption isotherm, the rate of mass transfer, the gas flow rate and the adsorbent particle size. Clearly, slow kinetics and unfavorable adsorption equilibrium result in long MTZ lengths which increases adsorber bed size.

The mass transfer coefficients for adsorption of the various trace impurities were estimated from transient uptake curves. The derivation of the kinetic model is given in Appendix B. Once mass transfer coefficients were determined for a given adsorbate/adsorbent system, the mass transfer zone length was estimated by a technique developed by Rosen (5). This technique for estimating MTZ lengths and the kinetic model derived in Appendix B both assume that adsorption isotherms are linear. Linear adsorption isotherms produce MTZ's that spread out as they progress through the adsorption column. Many of the isotherms for catalyst poison removal are not linear, but rather concave to the concentration axis. This type of adsorption isotherm produces MTZs

that sharpen as they proceed through the column. Thus, the linear isotherm assumption, which was made for simplicity, will over predict MTZ lengths.

For a symmetrical mass transfer zone, the length of the zone is given by the equation:

$$MTZ = 2 [1 - t_1/t_m] L$$

where  $t_1$  is the time to initial breakthrough,  $t_m$  is the time to the midpoint of breakthrough and  $L$  is the column length. Therefore, estimation of MTZ lengths requires values for  $t_1$ ,  $t_m$ , and  $L$ . The midpoint to breakthrough is calculated from the mass balance on the column using the equation:

$$t_m = L \rho_b K_H / G$$

where  $L$  is the bed length (ft),  $\rho_b$  is the bulk density of the adsorbent (lbs/ft<sup>3</sup>),  $K_H$  is the Henry's law constant for adsorption (lbmoles/lb) and  $G$  is the gas flow rate (lbmoles/ft<sup>2</sup>/hr). After  $t_m$  is calculated for a given bed length, then  $t_1$  is calculated from Rosen's solution using the equation:

$$t_1 = t_m - 2X (t_m/K)^{1/2}$$

where  $K$  is the mass transfer coefficient in units of reciprocal time and  $X$  is a factor that takes into account the initial and final impurity concentration.

### Sample Design Calculation

Estimation of column length of H-Y zeolite needed for removal of 5 ppm  $\text{Fe}(\text{CO})_5$  is given below. The design is based on an adsorption temperature of  $75^\circ\text{F}$ , 450 psig total pressure, and a G-rate of  $10 \text{ lbmoles}/\text{ft}^2/\text{hr}$ . The Henry's law constant for  $\text{Fe}(\text{CO})_5$  adsorption under these conditions is estimated from mixed Langmuir considerations to be  $15 \text{ lbmoles}/\text{lb}$ . The experimental value at  $75^\circ\text{F}$  and 90 psig carrier is  $30 \text{ lbmoles}/\text{lb}$  ( $0.15 \text{ mibmoles}/\text{lb}/5 \text{ ppm}$ ). The mass transfer coefficient determined from lab data is  $46.3 \text{ hr}^{-1}$ . The value of  $k$  determined from Appendix B is in units of  $\text{lbmole}/\text{lb}/\text{min}$ . To get  $k$  in units of reciprocal time, division by the Henry's law constant is necessary. Assuming the inlet  $\text{Fe}(\text{CO})_5$  concentration is 5 ppm and the outlet is 0.01 ppm, the value of  $X$  is 2.0. The bulk density of H-Y zeolite is  $40 \text{ lbs}/\text{ft}^3$ . MTZ lengths calculated for various bed lengths are given below:

<u>L (ft)</u>	<u><math>t_n</math> (hr)</u>	<u><math>t_1</math> (hr)</u>	<u>MTZ (ft)</u>
1.0	60.0	55.4	0.15
0.5	30.0	26.8	0.11
0.25	15.0	12.7	0.08

These calculations indicate that a column length of 0.5 ft will demonstrate initial breakthrough of  $\text{Fe}(\text{CO})_5$  after 27 hours on-stream. Similar calculations were done for  $\text{Ni}(\text{CO})_4$ , COS,  $\text{H}_2\text{S}$ , and HCl removal. The value needed for these calculations are given in the following table:

<u>Adsorbent</u>	<u>Poison</u>	$\frac{(\text{lbmoie/lb})}{K_H}$	$\frac{(\text{hr}^{-1})}{k}$	$\frac{(\text{lbs/ft}^3)}{P_b}$	$\Delta$
BPL	$\text{Ni}(\text{CO})_4$	24	5.6	30	1.7
FCA	COS	3.8	2.8	30	2.1
BASF S3-85	$\text{H}_2\text{S}$	400	0.10	80	2.0
BASF S3-85	HCl	1000	0.20	80	2.5

Using these values, the following pilot unit design was achieved:

Bed 1: BASF S3-85 for adsorption of  $\text{H}_2\text{S}$  and HCl in a throw-away system. Calculations suggest that under the conditions specified above, a 0.5 ft bed of BASF S3-85 should last about 50 days with inlet concentrations of 20 and 5 ppm for HCl and  $\text{H}_2\text{S}$ , respectively.

Bed 2: H-Y zeolite for removal of  $\text{Fe}(\text{CO})_5$ . A 0.5 ft bed is estimated to last 27 hours on-stream as indicated previously. Thermal regeneration in  $\text{N}_2$  at 250°F is required for reactivation.

Bed 3: BPL carbon for removal of  $\text{Ni}(\text{CO})_4$ . A 0.5 ft bed is estimated to last 29 hours on-stream. Thermal regeneration in  $\text{N}_2$  at 250°F is required for reactivation. These calculations assume an inlet concentration of 1 ppm and an outlet of 0.01 ppm.

Bed 4: FCA carbon for removal of COS. A 3.5 ft bed is estimated to last 25 hours on-stream. Thermal regeneration in  $\text{N}_2$  at 500°F is required for reactivation. These calculations assume an inlet concentration of 10 ppm and an outlet of 0.01 ppm.